

Filtering of Poisson Noise in Digital Mammography Using Local Statistics and Adaptive Wiener Filter

Marcelo A.C. Vieira¹, Predrag R. Bakic², Andrew D.A. Maidment²,
Homero Schiabel¹, Nelson D.A. Mascarenhas³

¹ Electrical Engineering Department, University of São Paulo, São Carlos, Brazil
{mvieira, homero}@sc.usp.br

² Department of Radiology, University of Pennsylvania, Philadelphia, USA
{predrag.bakic, andrew.maidment}@uphs.upenn.edu

³ Computer Department, Federal University of São Carlos, São Carlos, Brazil
nelson@dc.ufscar.br

Abstract. A novel image denoising algorithm has been proposed for quantum noise reduction in digital mammography. The method uses the Anscombe transformation to stabilize noise variance and convert the signal-dependent Poisson noise into an approximately signal-independent Gaussian additive noise. In the Anscombe domain, noise is removed through an adaptive Wiener filter, whose parameters are obtained considering local image statistics. Thus, the method does not require any *a priori* knowledge about the original signal, because all the necessary parameters are estimated directly from the noisy image. The method was applied on synthetic mammograms generated based upon an anthropomorphic software breast phantom with different levels of simulated quantum noise. The evaluation of the proposed method was performed by calculating the peak signal-to-noise ratio (PSNR) and the mean structural similarity index (MSSIM) before and after denoising. Results show that the proposed algorithm improves image quality by reducing image noise without significantly affecting image sharpness.

Keywords: Digital mammography, quantum noise, image denoising, Anscombe transformation, Wiener filter.

1 Introduction

Full Field Digital Mammography (FFDM) is currently the standard tool for breast imaging and is gradually replacing screen-film mammography as the preferred tool for breast cancer screening [1]. However, mammographic interpretation is a complex task, preventing radiologists from the ideal of detecting all abnormalities visualized on mammograms. Among the lesions evaluated in mammographic reading, special attention is given to clustered microcalcifications because they may represent the only sign of malignancy [2]. Due to their small size and the confounding effects of image noise, the visibility of microcalcifications may sometimes be relatively poor. Image quality significantly influences the performance of radiologists in mammography

interpretation. Thus, high quality mammograms are required for accurate detection and characterization of suspicious lesions in breast cancer screening.

In this context, image processing algorithms have been utilized to increase the visibility of microcalcifications, with the hope of improving the performance of radiologists [3]. However, for proper use of preprocessing techniques in mammographic images, some important aspects must be considered. First, use of image processing algorithms for the enhancement of high-frequency components, such as microcalcifications, has the undesirable effect of increasing the image noise [4]. On the other hand, image processing for noise suppression typically reduces sharp transitions between pixel intensities, which results in image blurring. This could impair the detection of fine detail and small structures in the breast image.

Denosing techniques are, in general, based on the assumption that noise is additive and signal independent (that is, there is no correlation between pixel values and the values of noise components) [4]. However, mammography images are acquired using the minimum radiation dose consistent with ensuring both adequate image quality and patient safety; as such, the quantum noise should be apparent. Quantum noise is non-additive and signal-dependent (that is, noise components values are correlated with respect to the radiation intensity). A recent study has shown that quantum noise is the dominant image quality factor in mammography and exerts greater influence than spatial resolution for the tasks of detecting microcalcifications and discrimination of masses by radiologists. A failure to address noise issues can impede diagnostic performance [5].

We propose a novel image denoising algorithm for quantum noise reduction in digital mammography, aimed at improving image quality, and consequently improving radiologists' performance in clinical interpretation. The method uses the Anscombe transformation [6] to stabilize noise variance and convert the signal-dependent quantum noise into an approximately signal-independent Gaussian additive noise. In the Anscombe domain, image noise is removed through an adaptive Wiener filter, whose parameters are obtained considering local image statistics. Thus, the method does not require any *a priori* knowledge of the original signal, because all the necessary parameters are estimated directly from the noisy image.

2 Methods and Materials

The following model describes the image degradation process during acquisition [4]:

$$g(x, y) = f(x, y) * h(x, y) + n(x, y) \quad (1)$$

where $g(x, y)$ is the degraded image, $f(x, y)$ is the input image, $h(x, y)$ is the degradation function, $n(x, y)$ is the additive noise and the operator “*” indicates convolution.

Restoration techniques usually manipulate this equation to obtain an estimate, $\hat{f}(x, y)$, of the input image when $h(x, y)$ and $n(x, y)$ are known. The additive noise $n(x, y)$ is incorporated by the digitization process and can be modeled as signal-independent Gaussian noise. However, $f(x, y)$ cannot be considered a noise-free image

because mammographic images are also corrupted by quantum noise, which is a non-additive noise and is normally modeled by a Poisson statistical distribution.

The Anscombe transformation is a variance-stabilizing transformation that converts a random variable with a Poisson distribution into a variable with an approximately additive, signal-independent Gaussian distribution with zero mean and unity variance [6,7]. Let the degraded image, $g(x,y)$, be the random variable. The Anscombe transformation of $g(x,y)$ is given by [6]:

$$z(x, y) = 2\sqrt{g(x, y) + \frac{3}{8}}. \tag{2}$$

This equation can be represented by the following additive model [7]:

$$z(x, y) = \left(2\sqrt{u(x, y) + \frac{1}{8}}\right) + v(x, y), \tag{3}$$

where $u(x,y)$ is the rate of the Poisson distributed image (i.e., the expected value) and $v(x,y)$ is the additive term, which is independent of the signal $s(x,y)$ and has an approximately Gaussian distribution.

After the Anscombe transformation, the additive term $v(x,y)$ includes both the quantum noise converted into Gaussian noise and the electronic white noise, originally incorporated by the digitization process. Thus, this transformation allows the use of any well-known denoising technique to reduce Gaussian additive noise by working on the image $z(x,y)$ in the Anscombe domain [7].

In this work, we use the adaptive Wiener filter to obtain an estimate, $\hat{s}(x, y)$, of the expected noise-free mammographic image in the Anscombe domain [7]. The Wiener filter calculates an estimate of a noise-free image that minimizes the mean squared error. Specifically, when $z(x,y)$ is assumed to have a Gaussian additive noise with zero mean, the Wiener filter is the optimal filter and has the following expression:

$$\hat{s}(x, y) = \bar{s} + \frac{\sigma_s^2}{\sigma_s^2 + \sigma_v^2} [z(x, y) - \bar{z}], \tag{4}$$

where \bar{s} and σ_s^2 are the mean and variance of the signal, respectively; \bar{z} is the mean of the image $z(x,y)$; and σ_v^2 is the variance of the noise.

In the Anscombe domain, we can assume that σ_v^2 is equal to 1. Moreover, \bar{z} is equal to \bar{s} because the mean of the noise, \bar{v} , is equal to zero [7]. Thus, we can rewrite the equation (4) as follows:

$$\hat{s}(x, y) = \bar{s} + \frac{\sigma_s^2}{\sigma_s^2 + 1} [z(x, y) - \bar{s}]. \tag{5}$$

Parameters \bar{s} and σ_s^2 can be estimated by local statistics of a preliminary estimate of the signal in the Anscombe domain, $\hat{\hat{s}}(x, y)$. We considered a square neighborhood of variable size around the pixel being processed. The preliminary estimate of the signal, $\hat{\hat{s}}(x, y)$, was obtained by blurring the image $z(x,y)$ with an averaging filter mask of size 3×3 [4].

After the adaptive Wiener filtering procedure, the inverse Anscombe transformation is applied to obtain the estimate, $\hat{u}(x, y)$, of an approximately noise-free mammographic image in the spatial domain. The inverse Anscombe transformation is given by the following equation [7]:

$$\hat{u}(x, y) = \frac{1}{4} \hat{s}(x, y)^2 - \frac{1}{8}. \quad (6)$$

3 Results

The assessment of the proposed denoising algorithm was performed considering synthetic mammograms generated based upon an anthropomorphic software breast phantom [8] with a cluster of microcalcifications with 50% and 25% of normal contrast. The contrast of the microcalcifications is specified as the relative linear x-ray attenuation coefficient compared to the tabulated attenuation of hydroxyapatite. All mammograms were generated using three different levels of quantum noise, simulating the normal clinical dose, half of the normal dose and a quarter of the normal dose. All of the images were restored using the proposed filter.

In order to evaluate the performance of the proposed methodology, we calculated two widely used image quality parameters: the peak signal-to-noise ratio (PSNR) [9] and the mean structural similarity index (MSSIM) [10]. Ideal mammograms without quantum noise were also generated to provide the ground-truth reference. These parameters were measured in full mammographic images (4096×1792 pixels) and two regions-of-interest (ROI) of 256×256 pixels containing, respectively, microcalcification clusters with 50% contrast and 25% contrast.

Figure 1 shows one example of the results obtained with the denoising algorithm on the synthetic images. The image on the left shows a ROI with a cluster of microcalcification with 50% of contrast extracted from the mammogram generated with a quantum noise correspondent to a quarter of normal clinical dose. In the center is the same image after denoising and on the right is the ideal image used as reference.

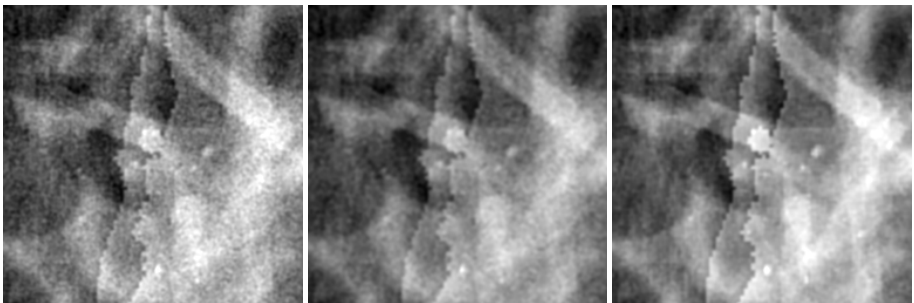


Fig. 1. ROIs (256×256) of a cluster of microcalcifications with 50% of contrast extracted from the mammogram generated with a quantum noise correspondent to a quarter of normal clinical dose. Left: noisy image; center: restored image; right: ideal image without noise.

Table 1 shows the PSNR and MSSIM measurements obtained with the proposed denoising algorithm for the synthetic FFDM images before and after denoising. The relative improvement of image quality achieved using the denoising methodology was also calculated. Figure 2 and Figure 3 show, respectively, the improvement in PSNR and MSSIM measurements after denoising as a function of the radiation dose.

Table 1. Results of PSNR and MSSIM measured for the proposed algorithm before and after denoising. Synthetic mammograms were generated with quantum noise corresponding to 100%, 50% and 25% of the normal clinical dose. Parameters were measured in the full mammographic images and two ROIs of 256 × 256 pixels containing, respectively, microcalcification clusters (MC) with 50% and 25% contrast. The relative improvement on image quality after denoising was also calculated.

Phantom Images		PSNR(dB)			MSSIM		
		Before	After	Improve-ment(dB)	Before	After	Improve-ment (%)
100% of the normal clinical dose	Full image	51.30	60.84	9.54	0.9921	0.9993	0.73
	ROI with 50% MC contrast	40.13	44.92	4.79	0.9329	0.9815	5.21
	ROI with 25% MC contrast	40.02	44.84	4.82	0.9317	0.9814	5.33
50% of the normal clinical dose	Full image	48.33	57.98	9.65	0.9845	0.9987	1.44
	ROI with 50% MC contrast	36.81	42.12	5.31	0.8728	0.9751	11.72
	ROI with 25% MC contrast	36.93	42.28	5.35	0.8741	0.9755	11.60
25% of the normal clinical dose	Full image	45.36	54.90	9.54	0.9702	0.9975	2.81
	ROI with 50% MC contrast	33.50	38.20	4.70	0.7776	0.9640	23.97
	ROI with 25% MC contrast	33.54	38.31	4.77	0.7771	0.9640	24.05

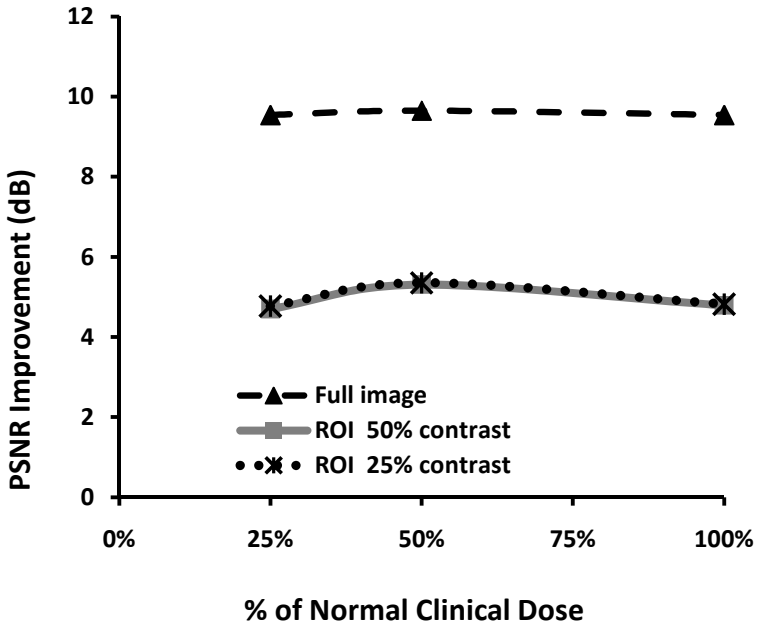


Fig. 2. Improvement in the PSNR measurements after denoising as a function of dose

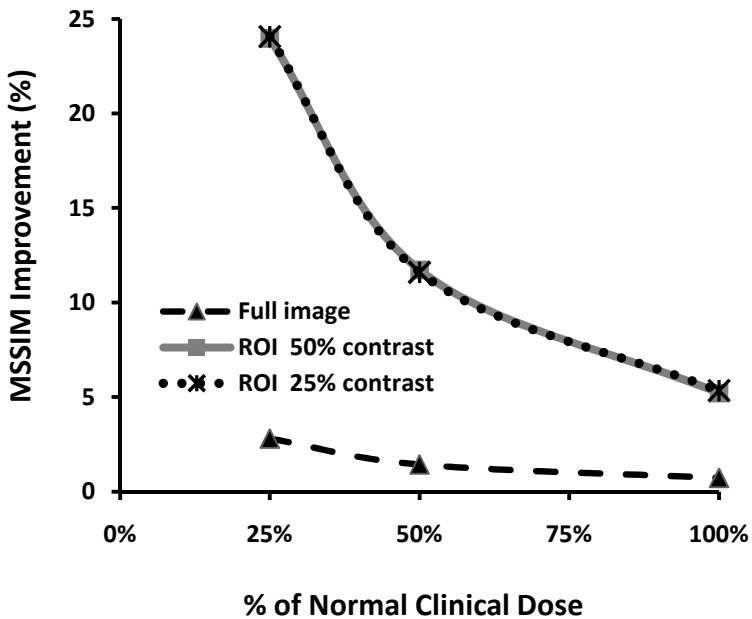


Fig. 3. Improvement in the MSSIM measurements after denoising as a function of dose

4 Discussion

In this work we investigated the use of the Anscombe transformation and the adaptive Wiener filter to reduce the quantum noise of digital mammography images. Improvement on mammographic image quality resulting from the proposed denoising method was evaluated. First, we compared the noisy and the reference images in terms of two widely used signal fidelity index: PSNR and MSSIM. As expected, it was found that images acquired at lower dose levels resulted in lower image quality index values, as shown in Table 1. This indicates that mammography quantum noise is signal-dependent and increases with a reduction in radiation dose, as expected.

In order to evaluate the proposed denoising methodology, the same image quality metrics were measured again after denoising, considering both the restored and the reference images. Results showed that the proposed filter improved image quality index values, as shown in Table 1. Increases of up to 9.65 dB in the PSNR and up to 24% in the MSSIM measurements were observed. This indicates that the proposed denoising filter produced restored images which accurately preserved the detail seen in the noise-free reference images. It was noticed that the relative improvement on image quality after denoising, evaluated by means of the MSSIM, was higher for images with lower simulated dose (Figure 3). However, little variation on PSNR measurements was observed as a function of the radiation dose (Figure 2).

Image quality assessment was also performed considering two ROIs of clustered microcalcifications extracted from the mammograms: one with 50% of contrast and one of 25% of contrast. Results suggested that the proposed methodology produced better quality images by reducing noise without noticeably affecting image sharpness, as seen at Figure 1.

In future work we will study the effect of the proposed denoising filter on the performance of microcalcification detection using observer studies and ROC analysis, in order to evaluate the clinical use of the proposed methodology in breast-cancer screening.

Acknowledgements. The authors would like to thank FAPESP and CAPES for their financial support and Ms. Susan Ng from *Real-Time Tomography* (Villanova, PA) for processing the simulated projection images.

References

1. Karellas, A., Vedantham, S.: Breast cancer imaging: a perspective for the next decade. *Med. Phys.* 35(11), 4878–4897 (2008)
2. Acha, B., Serrano, C., Rangayyan, R.M., Leo Desautels, J.E.: Detection of microcalcifications in mammograms using error of prediction and statistical measures. *J. Electron. Imaging* 18(1), 013011 (2009)
3. Papadopoulos, A., Fotiadis, D.I., Costaridou, L.: Improvement of microcalcification cluster detection in mammography utilizing image enhancement techniques. *Comput. Biol. Med.* 38(10), 1045–1055 (2008)

4. Gonzalez, R.C., Woods, R.E.: Digital Image Processing, 3rd edn. Prentice Hall, Upper Saddle River (2008)
5. Saunders, R.S., Baker, J.A., Delong, D.M., Johnson, J.P., Samei, E.: Does image quality matter? Impact of resolution and noise on mammographic task performance. *Med. Phys.* 34(10), 3971–3981 (2007)
6. Anscombe, F.J.: The transformation of Poisson, binomial and negative-binomial data. *Biometrika* 35, 246–254 (1948)
7. Mascarenhas, N.D.A., Santos, C.A.N., Cruvinel, P.E.: Transmission tomography under Poisson noise using the Anscombe transformation and Wiener filtering of the projections. *Nucl. Instrum. Meth. A* 423, 265–271 (1999)
8. Bakic, P.R., Zhang, C., Maidment, A.D.: Development and characterization of an anthropomorphic breast software phantom based upon region-growing algorithm. *Med. Phys.* 38(6), 3165–3176 (2011)
9. Wang, Z., Bovik, A.C.: Mean squared error: Love it or leave it? A new look at signal fidelity measures. *IEEE Signal Proc. Mag.* 26(1), 98–117 (2009)
10. Wang, Z., Bovik, A.C., Sheikh, H.R., Simoncelli, E.P.: Image quality assessment: from error visibility to structural similarity. *IEEE T. Image Process.* 13(4), 600–612 (2004)